Supplementary Information

Table of contents

This supplementary information file includes 14 parts of content and 1 supplementary video (Movie S1).

1. The color changes in the process of ATIR

Figure S1. Photos of process from MRS to BDS. After absorbing precursor solution, MRS grew dark gradually and changed into black after 30min. BDS was taken to stand for 24h to make it react fully.

2. Reaction between chloroauric acid and sodium citrate in aqueous solution and ambient temperature

To eliminate the effect of MRS, the reaction between chloroauric acid and sodium citrate was conducted in aqueous solution and ambient temperature. As shown in Figure S2, three reaction systems of different concentrations were used. The solution of original concentration grew black and precipitate gradually. Solutions of 1/10 and 1/100 of original concentration can form stable colloids,and the color of high-concentration solution is deeper. UV-Vis spectrum were tested and the peaks at around 530nm belongs to GNPs colloids. This is the first time to report the reaction between chloroauric acid and sodium citrate in ambient temperature without UV irradiation, X-rays or γ-rays.
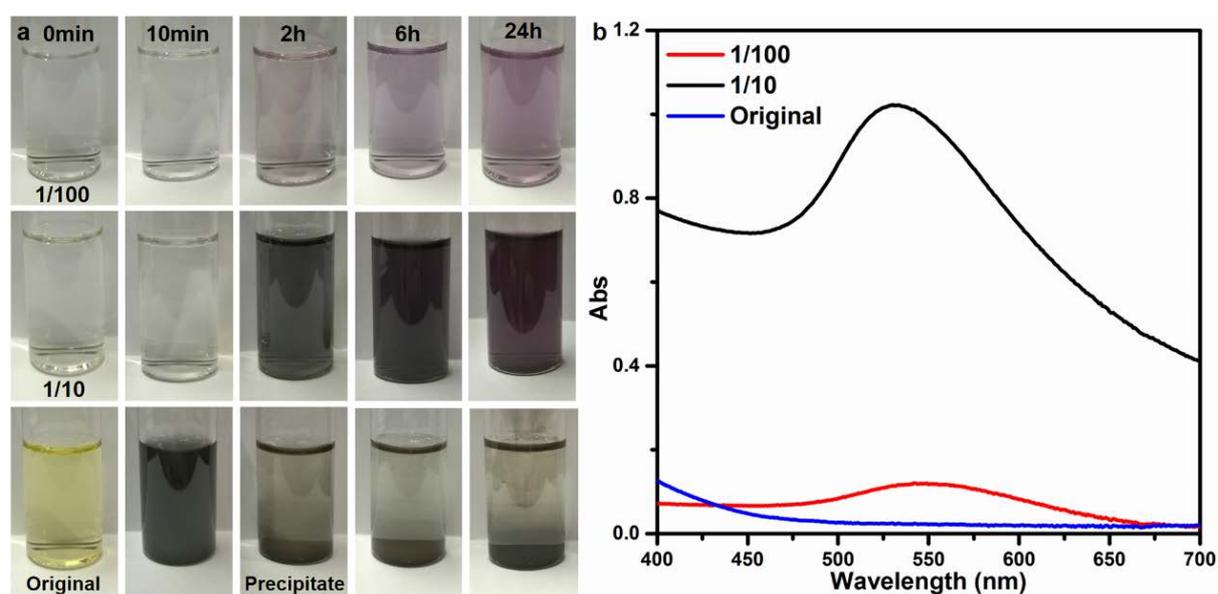
Figure S2. (a) Photos of three aqueous solution after reacting for 24h. Original represents that the concentration of chloroauric acid and sodium citrate are identical with ATIR method used in main text, and 1/10 and 1/100 means the original solution was diluted by 10 and 100 times. (b) UV-Vis spectra of three aqueous solutions.

3. Flexibility of BDS
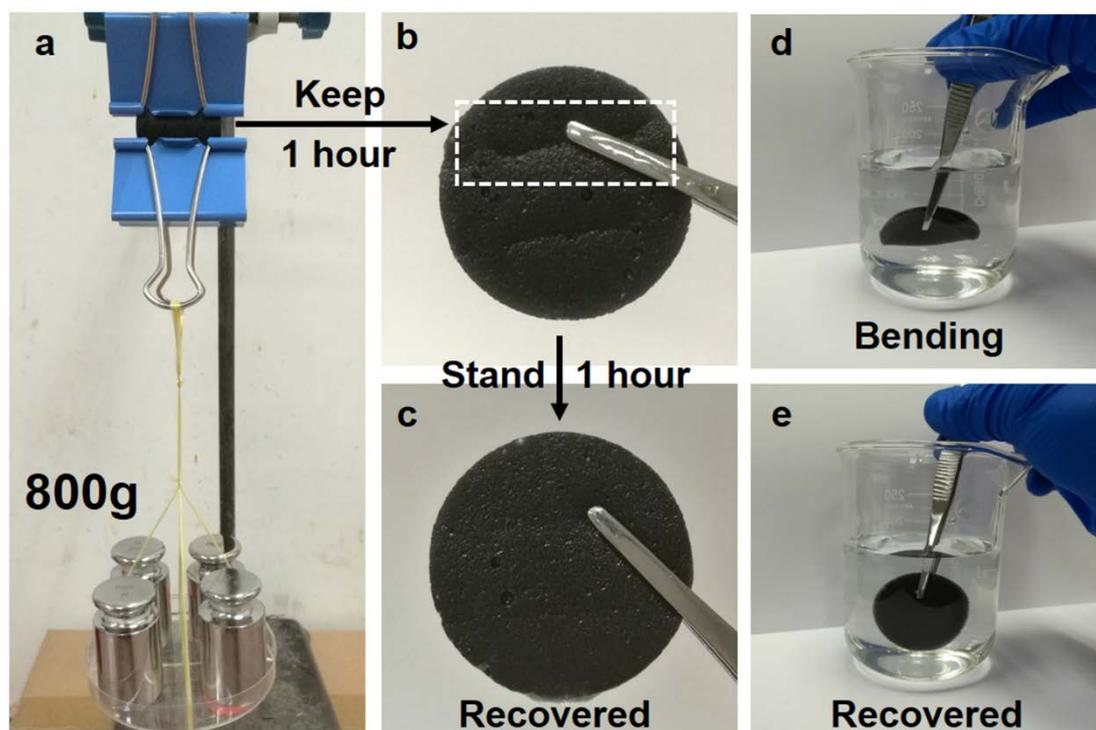
Figure S3. (a-c) Sketching test of BDS. After sketching for 1 hour under the weight of 800 g, no fracture was observed in BDS, but obvious trace which caused by pressure of clips appeared on BDS. Such trace can recover itself by standing for 1 hour. (d-e) Bending test of BDS. These tests proved that BDS possesses excellent flexibility, which make BDS hard to be damaged during use.

4. Water absorbing ability of MRS

A MRS column was dried completely and then was weighed at once. Then, made such MRS soaked with DI water and weighed the MRS. Details were shown below:

Dried MRS: 0.2187g
Soaked MRS: 23.5848g
Water absorbing capacity: 23.3661g
Volume of MRS: 23.94 cm^3 (diameter: 3.3cm, height: 2.8cm)
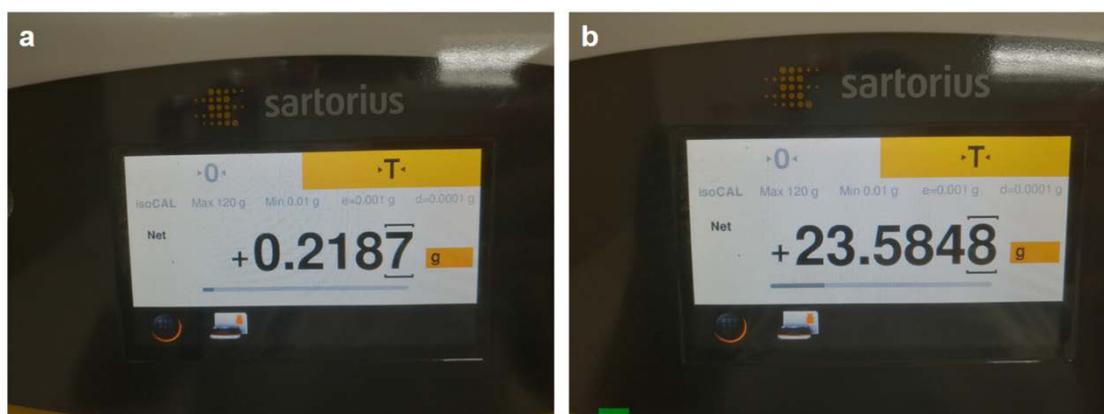
Figure S4. The weight of MRS before (a) and after (b) absorbing water.

5. Pore size and area of MRS
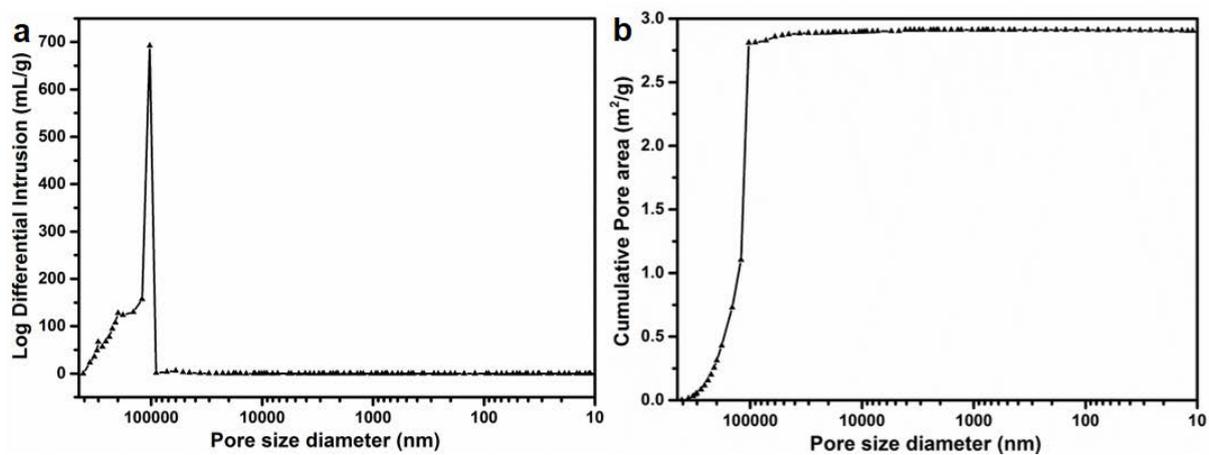
Figure S5 (a) Pore-size distribution curve of MRS. (b) The curve of cumulative pore area versus pore size diameter.

6. Density of GNPs loading in BDS

Three MRS columns were dried completely and weighed at once. Then, made these MRSs change into BDSs by ATIR method, followed by drying and weighing them. Details were shown below:

MRS columns: 0.6189g
After ATIR process: 0.6755g
Weight change (weight of GNPs): 0.0566g
Total volume of MRS: 71.81cm^3
Density of GNPs loading in BDS: 0.00079 g cm^{-3}
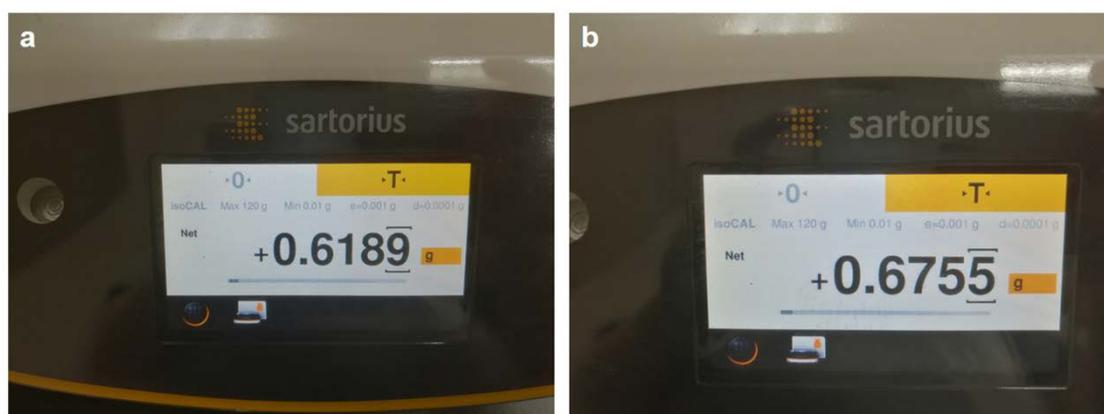
Figure S6. Weight of MRS (a) and BDS (b) prepared by ATIR method.

7. The reflectance and transmittance of BDS with different thickness

According to results below, thicker BDS features lower transmittance than thinner one (when thickness < 4mm), and thus increases solar absorption.
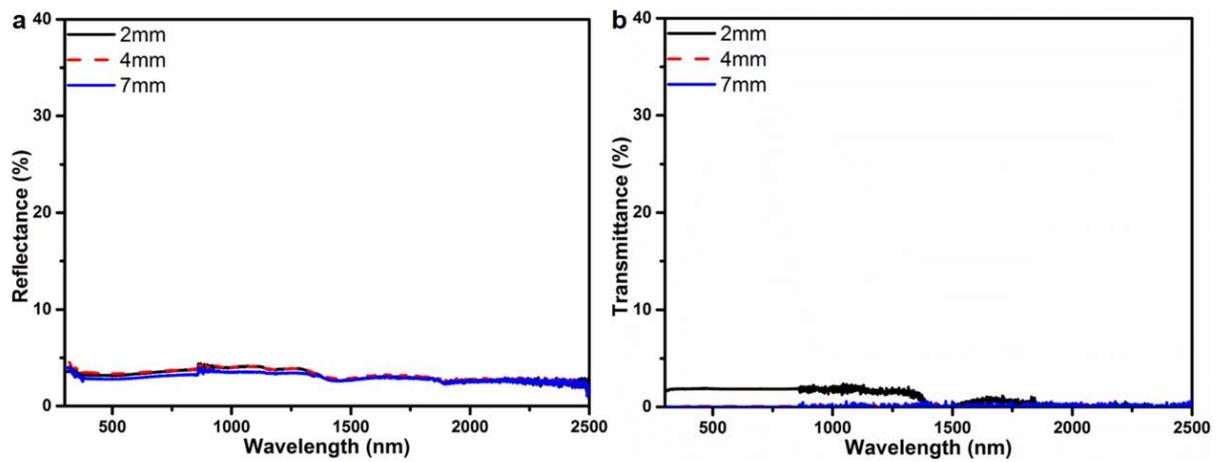
Figure S7. (a) The reflectance of BDS with thickness of 2mm, 4mm and 7mm. (b) The transmittance of BDS with thickness of 2mm, 4mm and 7mm.

8. The result of removing solid salt by using GNP paper.

GNP paper was prepared by a plate thermal reduction method that have been reported by our team.[1] For comparing with BDS, such a GNP paper was placed on a MRS column with the same cross-section area as the test of BDS. GNP paper is a 2D membrane without 3D porous structure, which makes the move and exchange of solution much harder. As a result, most of solid salt still remained on GNP paper after being soaked for 60min. The results of controlled experiment proved that the 3D porous structure of MRS/BDS is key to the move and exchange of solution.
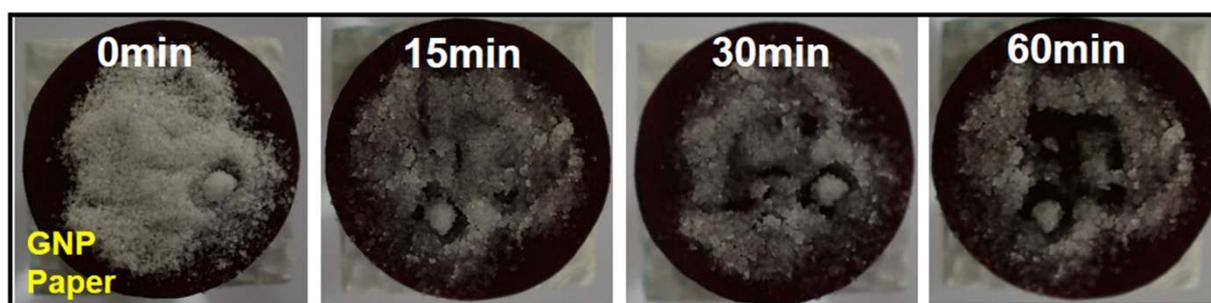
Figure S8. Photos of solid salt after being placed on soaked GNP paper.

9. Some parameters related to solar desalination property of BDS evaporator
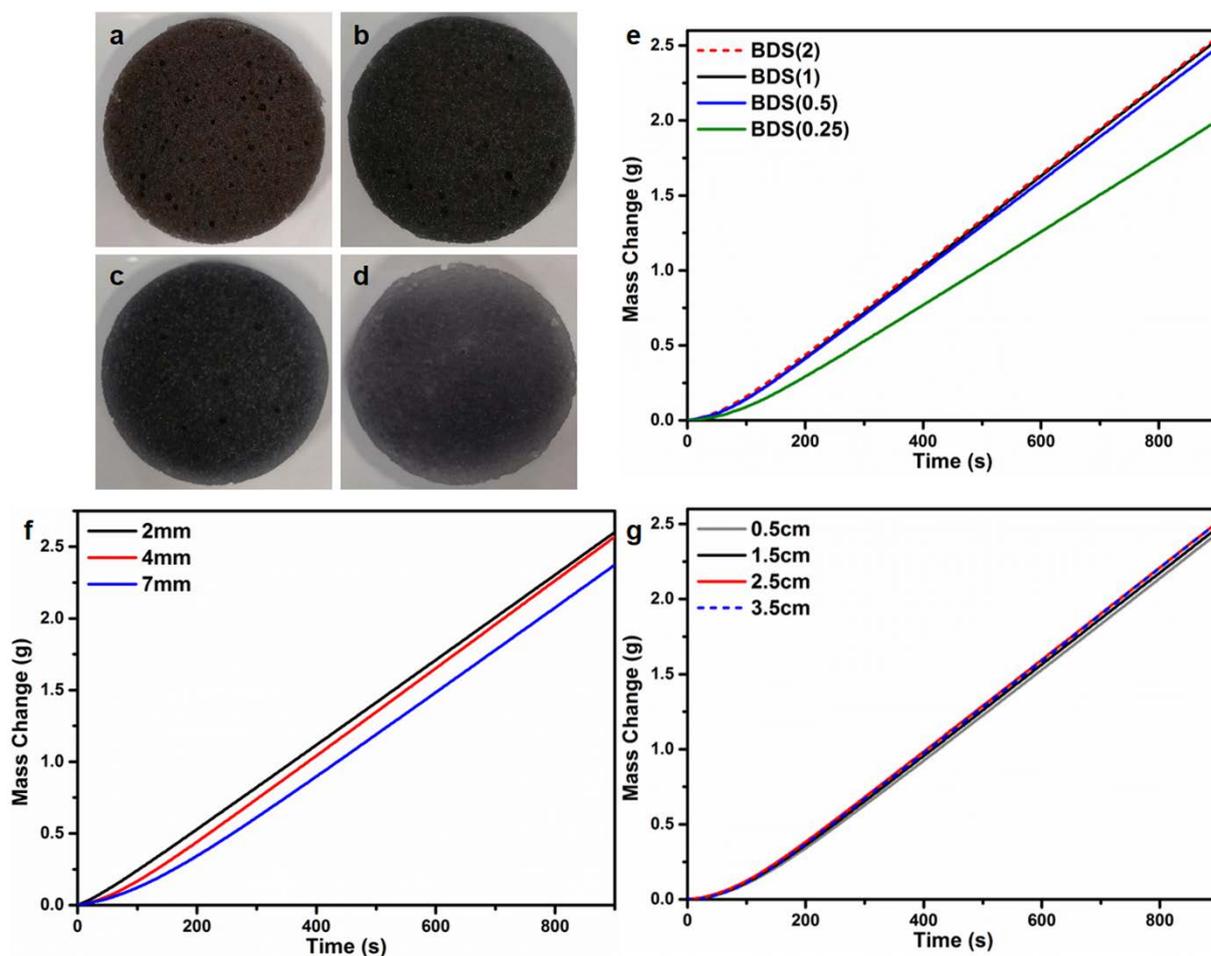
Figure S9 (a-d) Photos of BDS(2), BDS(1), BDS(0.5), BDS(0.25). (e-g) Mass change-time curve of BDSs with different GNPs density (f), different thickness (f), and the BDS evaporators using MRS pillars of different height.

To investigate the relationship between density of GNPs of BDS and solar desalination property, BDSs were prepared by using precursor solution with concentration 2, 1, 0.5, 0.25 times of the solution we used in manuscript, represented by BDS(2), BDS(1), BDS(0.5), BDS(0.25) respectively. The samples grew darker and darker with the dosage of precursor increasing, while BDS(2) shows slightly golden color, indicating some agglomeration of GNPs occurred (figure S8 a-d). Taking these samples to solar desalination tests, as figure S8e shown, from BDS(0.25) to BDS(1), the evaporation rate increased step by step, and the changes from BDS(1) to BDS(2) are very subtle. These results reveal that, within limits, the solar desalination property increases with the addition of GNPs loading density, while excessive GNPs loading does little help to solar desalination property.

The relationship between thickness of BDS and solar desalination property was investigated by conducting solar desalination tests of BDS with thickness of 2mm, 4mm and 7mm under 10 kW m^{-2}. The stable evaporation rates of these three samples were 12.50 kg m^{-2} h^{-1}, 12.84 kg m^{-2} h^{-1}, 12.33 kg m^{-2} h^{-1} respectively (figure S8f). The thin sample (2mm) reached stable evaporation rate faster, while the stable rate was a little lower than the thicker sample (4mm) due to its lower solar absorption (figure 2C). The 7mm-thick BDS reached stable much slower

and the stable rate was the lowest among these 3 samples. This result mainly because following two reasons: (1) Excessively thick sample is not helpful to increase solar absorption. (2) More water is stored in BDS when the sample is thicker, which needs to absorb more heat to reach surface thermal balance and weakens the surface heat localization effect. These results revealed that BDS in an appropriate thickness can balance the needs of solar absorption and surface heat localization and enable an efficient solar evaporation and desalination.

Then, the influence of the height of the MRS used in BDS evaporators were investigated by regulating the distance between lower surface of BDS and the surface of water. The evaporation rate were 12.75 kg m^{-2} h^{-1}, 12.84 kg m^{-2} h^{-1}, 12.87 kg m^{-2} h^{-1}, 12.96 kg m^{-2} h^{-1} when the height were 0.5 cm, 1.5 cm, 2.5 cm, 3.5 cm. Results shows that, under the premise of adequate water supply, the height of MRS has little influence on solar desalination property.

10. Mechanism of BDS evaporator to limit heat loss during salt resistant process.
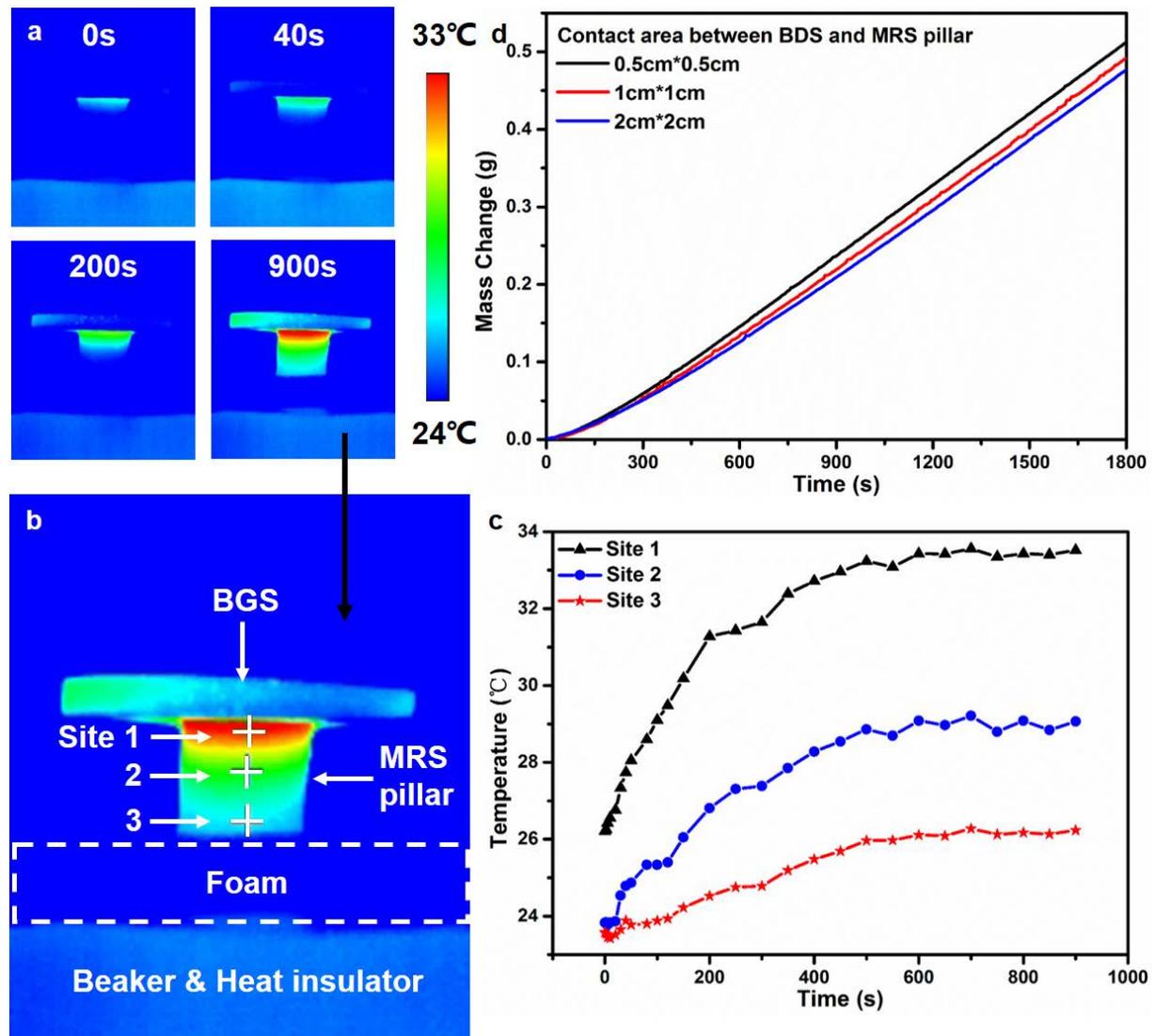
Figure S10. (a) Temperature variation and distribution of MRS pillar when evaporated under 1 kW m⁻². (b) Magnified IR camera image (900s) of figure S9a. (c) Temperature variation curve of site 1, 2 and 3, which were marked out in figure S9b. (d) Evaporation curves of BDS evaporators using MRS pillar with cross section area 0.25 cm², 1 cm² and 4 cm².

When the self-driven salt resistant mechanism works, hot concentrated solution flows down which will cause heat loss to bulk water. Considering that solutions flow down and are pumped up through the same path (MRS pillar), hot concentrated solution and cold dilute solution can encounter and exchange heat. Thus, the dilute solution can be preheated to limit heat loss. To observe this process, temperature variation and distribution of MRS pillar were recorded (Figure S10a-c). Temperature in MRS pillar distributed in gradient obviously, and decreased gradually from top to the bottom. After evaporating for 900s, temperature of site 1 (Figure S10b-c) increased by 7.3 ℃, while site 2 and 3 increased by 5.0 ℃ and 2.6 ℃ respectively. These results prove that, during the process of flowing down, hot concentrated solution transfers heat to cold solution along the MRS pillar, and finally goes into bulk solution at a much lower temperature. Meanwhile, the cold dilute solution is preheated to a much higher temperature

before it is supplemented to BDS. Thus, heat loss caused by the self-driven salt resistant mechanism is greatly limited.

To further prove the preheating process, MRS pillars with different cross section area were used in BDS evaporator for control experiments (use S+ Cross section area ($S_{0.25}$, S_1, S_4) to represent evaporators). Since hot concentrated solution flows away from BDS slower when using smaller MRS, cold dilute solution can be preheated more fully and enhancing the heat localization on evaporation surface. As shown in figure S10d, once illumination beginning, $S_{0.25}$ spend 300s to reach the balanced evaporation rate 1.26 kg m^{-2} h^{-1}, while S_1 spend 500s to reach 1.24 kg m^{-2} h^{-1} and S_4 spend 800s to reach 1.23 kg m^{-2} h^{-1}. Within limits, BDS evaporator with smaller MRS pillar exhibited faster acceleration of evaporation rate and higher balanced rate.

11. Temperature changes by using BDS without pin-like shape 10 kW m^{-2}

The temperature inside BDS increased by 21.3℃, and the temperature of bulk water increased by 7.8℃. Compared with datum of pin-like BDS evaporator, the reduction of heat loss can be proved.
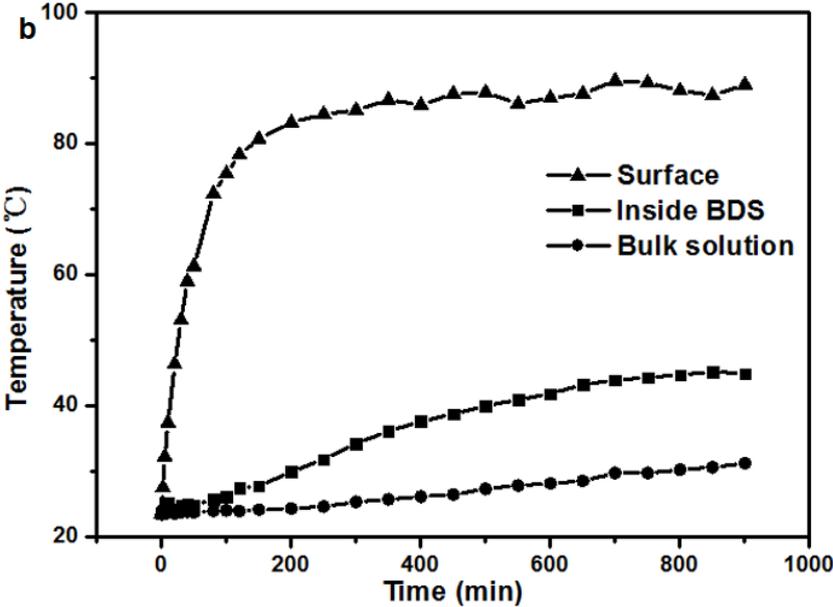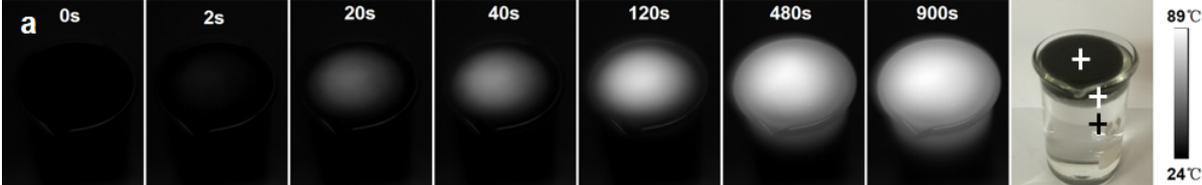
Figure S11. (a) IR-Camera images of BDS without pin-like shape during evaporation process. The crosses are the datum recording position of figure S6b (b) Temperature value of surface, sponge and bulk water in different time.

12. Details of 11-hours evaporation using BDS evaporator
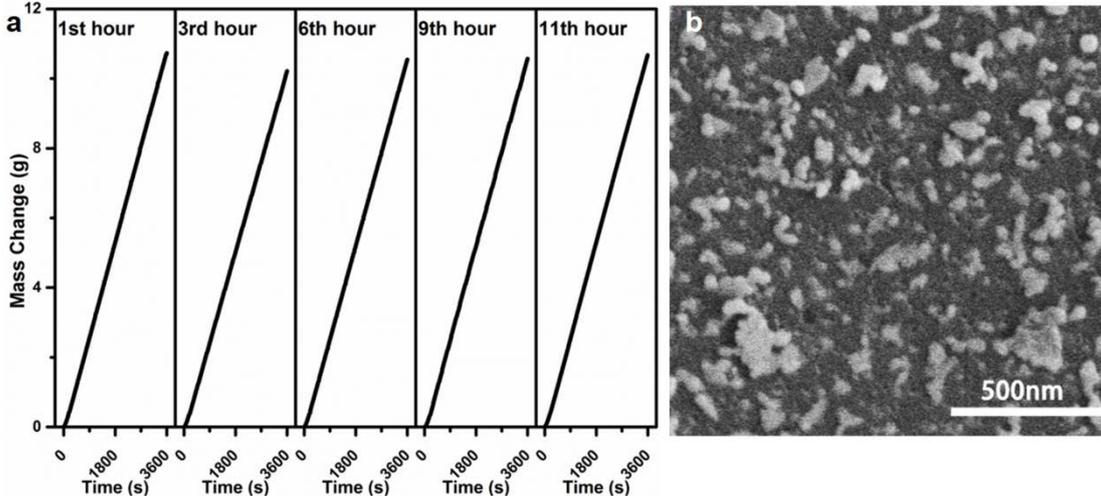
Figure S12. (a) Mass change curves of 1st, 3rd, 6th, 9th and 11th hour. (b) SEM image of BDS after evaporating for 11 hours, which shows no obvious change of surface morphology.

13. BDS after the treatment of HCl, NaOH solution and ultrasonic

BDSs were immersed in HCl solution (pH=1.2) and NaOH solution (pH=13.0) for about 16 hours. Another BDS was put into DI water to ultrasonic treatment for 2h.

Table S1. Changes of BDS after treatment above.

Item / Treatment	Solar absorption	Evaporation efficiency
Acid	-1.2%	-0.6%
Alkali	0%	0
Ultrasonic	+0.1%	-0.3%
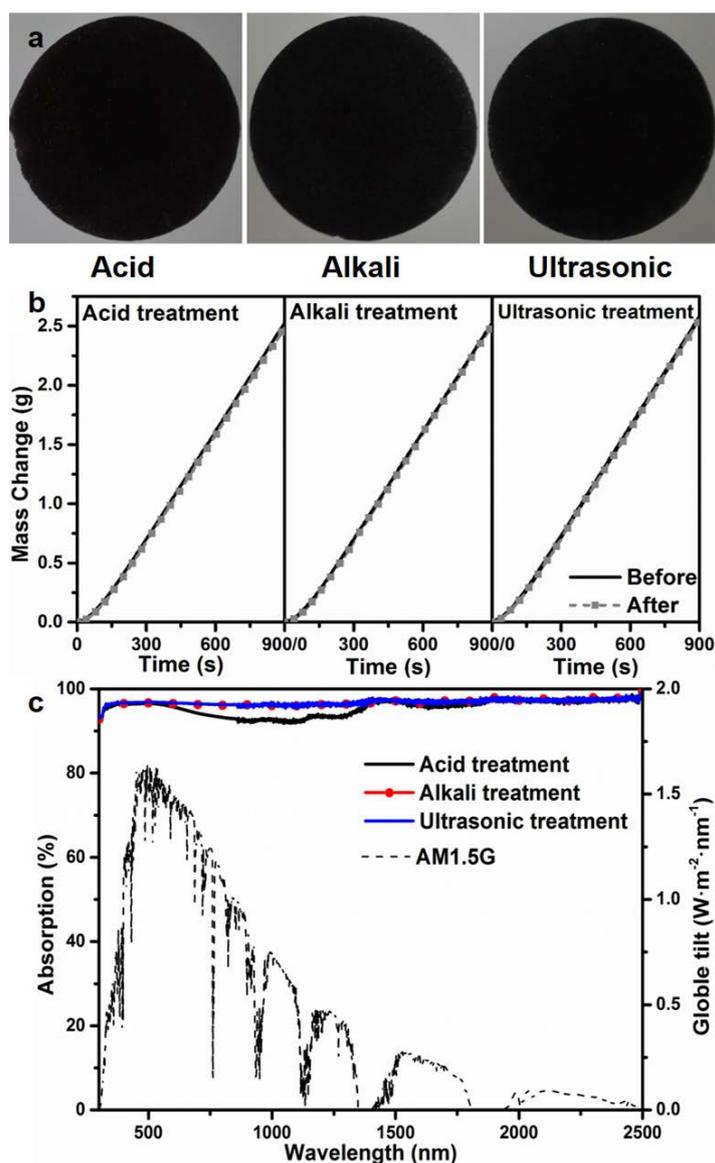
Figure S13. (a) Photos of BDS after treated. (b) The evaporation curve for 900s of BDSs before and after treatment. (c) The UV-Vis-IR spectrum of BDSs after treated.

14. Quality of collected fresh water by evaporating sea water from Shenzhen Bay.
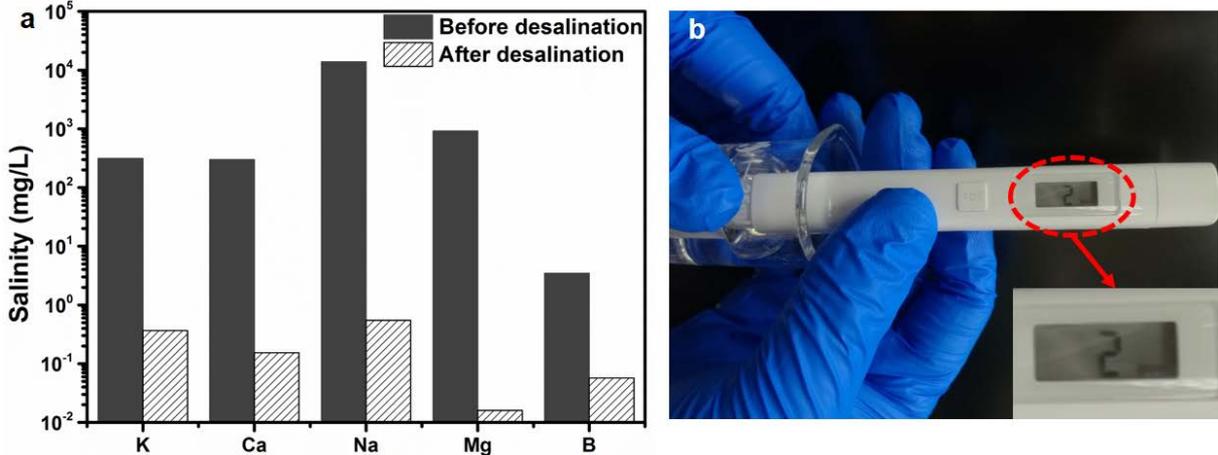
Figure S14. (a) The concentrations of five major ions of sea water in Shenzhen Bay before and after desalination. (b) TDS value of fresh water produced by evaporating sea water from Shenzhen Bay under natural sunlight. The TDS value was measured by the TDS detection device (Xiaomi Co., Ltd.).